

# Wind loading characteristics of super-large cooling towers

L. Zhao\* and Y.J. Ge

*State Key Laboratory for Disaster Reduction in Civil Engineering, Tongji University, Shanghai, China*  
(Received July 29, 2008, Accepted October 27, 2009)

**Abstract.** The aerodynamic and aero-elastic model tests of the China's highest cooling tower has been carried out in the TJ-3 Boundary Layer Wind Tunnel of Tongji University. By adopting a scanivalve system, the external wind pressure is firstly measured on 12×36 taps for a single tower, two and four grouped towers under the condition of both smooth flow and the boundary layer due to surrounding geographic and building topography. The measurements of internal wind pressure distribution of 6×36 taps are taken for a single tower under the various ventilation ratios ranging from 0% to 100% of stuffing layers located at the bottom of the tower. In the last stage, the wind tunnel tests with an aero-elastic model are carefully conducted to determine wind-induced displacements at six levels (each with eight points) with laser displacement sensors. According to the measurement results of wind pressure or vibration response, the extreme aerodynamic loading values of the single or grouped towers are accordingly analyzed based on probability correlation technique.

**Keywords:** cooling tower; tower group effect; wind-vibration factor; probability correlation.

---

## 1. Introduction

The collapse of three cooling towers at Ferrybridge power station in 1965 led to a series of investigation (Langhaar, *et al.* 1970, Cole, *et al.* 1975, Mungan 1976, Armitt 1980, Niemann 1980, Almannai, *et al.* 1981), involving quasi-static bending and dynamic analyses, transient dynamic response and stability analyses, aerodynamic and aero-elastic wind tunnel tests, etc. However, more than 40 years pass, the design of a newly built super-large cooling tower, featuring hyperbolic configuration and circle-shape section, is still in many cases governed by wind loading (Viladkar, *et al.* 2006, Waszczyszyn, *et al.* 2000, Noh 2006, Noorzaei, *et al.* 2006, Zahlten and Borri 1998). For design engineers, more attentions are usually focused on three aspects, namely surface pressure distribution, tower group factor and wind-vibration factor. By implementing simultaneous pressure-measured tests of cooling tower rigid model in the wind tunnel, mean and fluctuating wind pressure distributions over its external and internal surfaces can be obtained. With the assistance of wind tunnel tests on aero-elastic models, some information about wind-vibration factor can also be attained. In order to guide the design process effectively, equivalent static expressions on time-variant aerodynamic loads for cooling towers under special condition are required.

---

\* Corresponding Author, Associate Professor, E-mail: zhaolin@tongji.edu.cn

The effect of wind loads on adjacent cooling towers is usually simplified as 1.0 ratio factor under the assumption that the central distance of neighboring towers is equal or larger than 1.5 times the tower base diameter, and the tower height is less than 165.0 m in Chinese GB/T 50102-2003 (2003) and DL/T 5339-2006 (2006) Codes. However, in a practical engineering situation in the southeast China, a set of designing cooling towers are part of a dense arrangement of large buildings, which are of comparable size with the cooling towers. The tower distance conforms to the basic requirements of the Chinese Codes (see Fig. 1-2 and Table 1), moreover the tower height of 177.147 m also exceeds the minimum requirement of Chinese Codes. Actually, as for central distance of tower groups alone, wind loading Codes and guidelines vary among various countries, more or less differing in items (Orlando 2001, Sun and Gu 1995). Taking Chinese Codes (2003, 2006) and BTR (1990), for a central distance of 1.5 times the tower base diameter, the group factor is 1.0, while, however, in the French ‘Règles Professionnelles’ (1980), for a distance of 3.0 times tower base diameter, the group factor remains 1.0, for a distance of 2.0 it is 1.15. So, in special

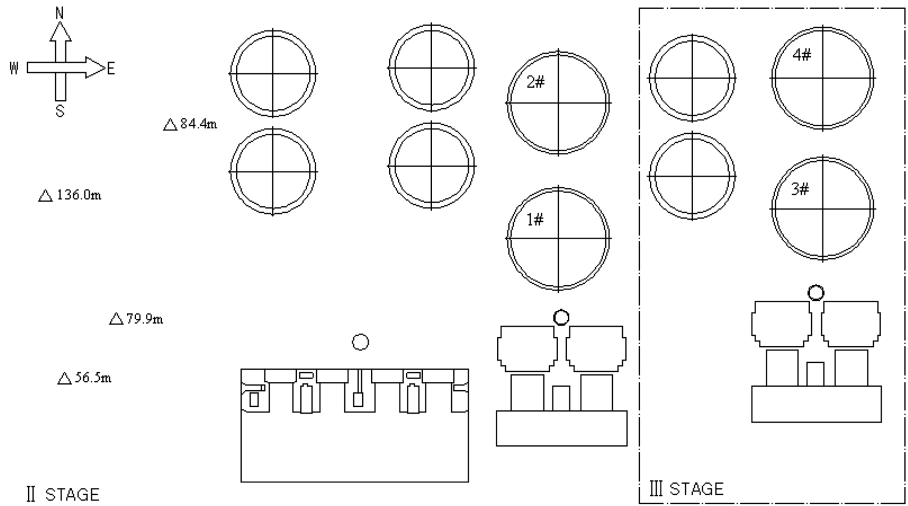


Fig. 1 Outline of cooling towers (1#-4#) and adjacent buildings for II and III construction stages

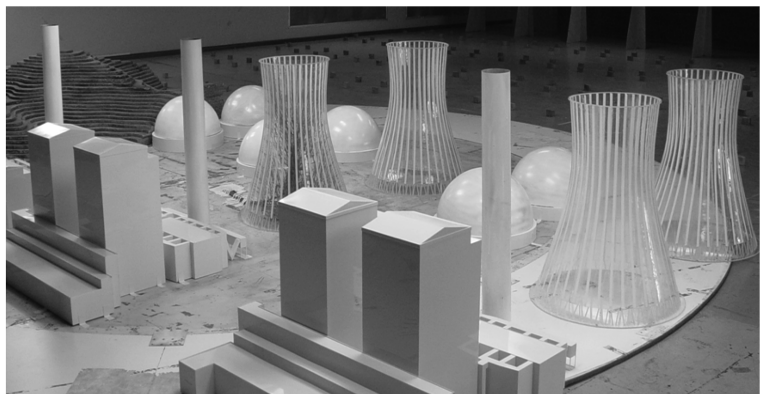


Fig. 2 Cooling towers and adjacent buildings in the wind tunnel (1:200)

Table 1 Buildings dimensions of electric power plant

Cooling tower height	177.147 m
Tower top diameter	82.260 m
Throat diameter	78.216 m
Tower base diameter	134.694 m
Minimum distance of towers	$\geq 1.5$ tower base diameter
Height of half sphericity bunker	80.0 m
Chimney height	210.0 m
Hill height	56.5~136.0 m
Other building height	35.0~135.0 m

cooling tower cases that exceed requirements of the Codes, as mentioned by Niemann and Köpper (1998), it's necessary to re-examine wind loading characteristics of cooling tower for the complicated configurations.

## 2. Aerodynamic and aero-elastic model tests

1:200 reduced scale models were selected considering upper limitation of the wind block ratio of working plate in TJ-3 wind tunnel. Fig. 3 shows three types of cooling tower models, specifically divided into the rigid models for internal (a) and external (b) wind pressure and aero-elastic model (c) for aerodynamic performance. The block ratio of test models in the wind tunnel is about 7%. The wind environment is Type A terrain. Wind environment about Terrain A in Chinese wind loading codes means that power exponent of vertical average wind profile at 10-min time interval is 0.12 and roughness length of ground surface is 0.05. More information can be referred from Fig. 4.

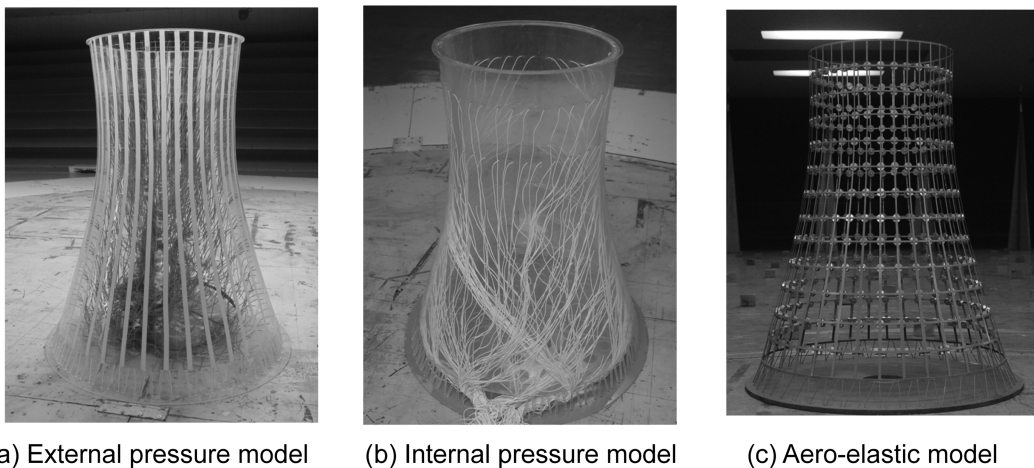


Fig. 3 Three types of reduced-scale models in the wind tunnel (1:200)

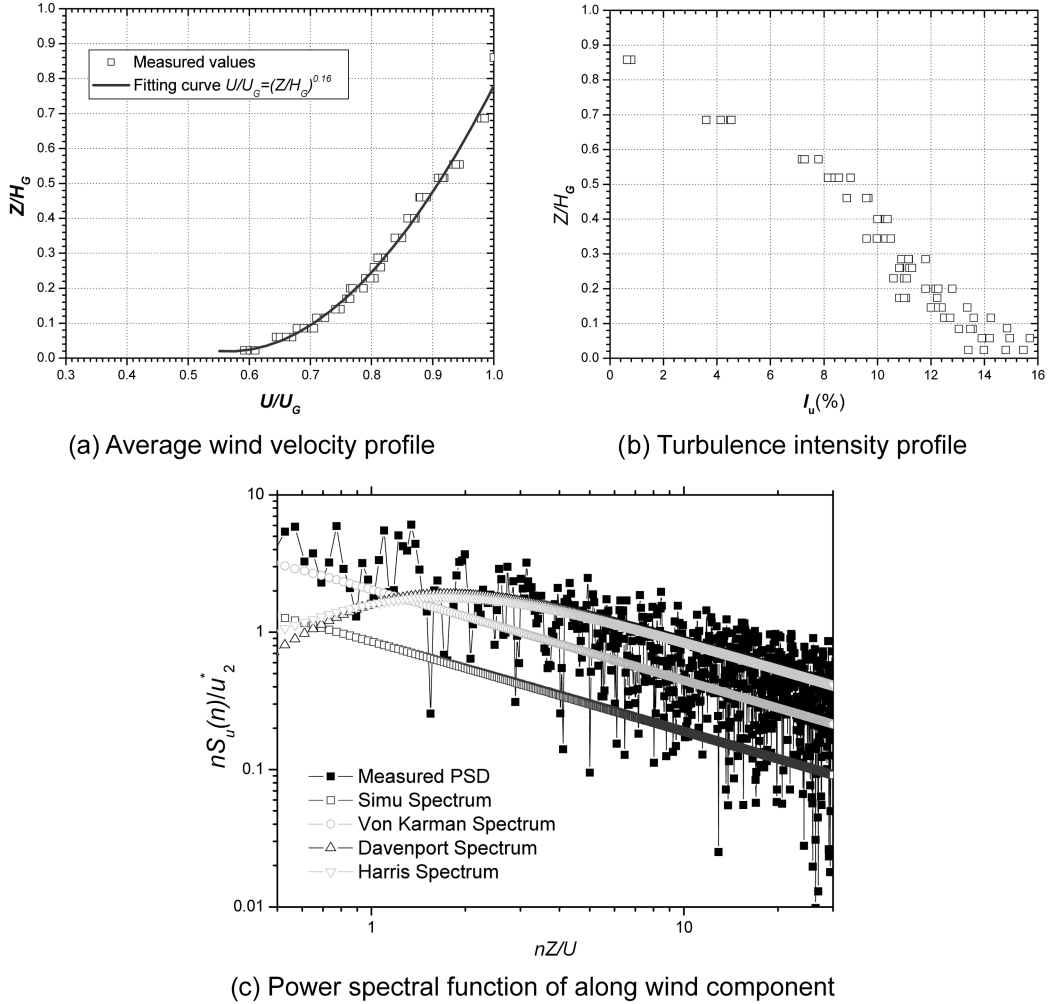


Fig. 4 Wind environment parameters of Type A terrain in TJ-3 wind tunnel

There are totally  $12 \times 36$  external pressure taps, distributed in 12 vertical sections, and in 36 horizontal circular directions for the external pressure model, see Fig. 5(b). The internal pressure model, totally  $6 \times 36$  internal pressure taps, includes 6 vertical sections and 36 horizontal circular directions for each section, see Fig. 5(c). The aero-elastic model mainly consists of  $14 \times 36$  spatial thin steel sheets, which provide reduced-scale stiffness and truly simulated bending, torsion and axis stiffness components by modifying three-dimensional sizes of each thin sheet, such as the depth  $d_i$ ,  $d_j$  and the width  $w_i$ ,  $w_j$  (see Fig. 6), and of  $12 \times 36$  pieces of copper additional masses, which simulate reduced-scale mass distribution. More design information of aero-elastic model can be referred in Table 2. The geometrical shape of the aero-elastic model is simulated with thin plastic membrane with less than 0.05 mm depth. There are 8 laser displacement sensors fixed on horizontal tray which can be moved along the vertical direction at 6 measurement heights. In Fig. 5(d), measured points for outside or inside wind pressure distribution and measured sections for wind-induced vibration response are illustrated. The front 5 natural frequencies of the model determined from spectral

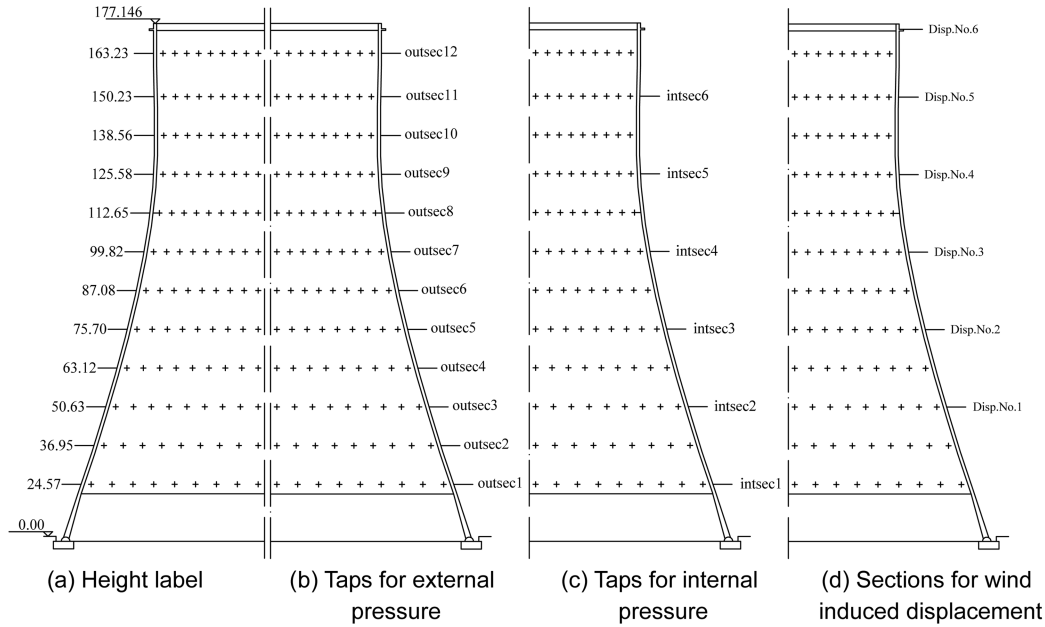


Fig. 5 Measured points of outside or inside wind pressure distribution and measured sections of wind-induced vibration response

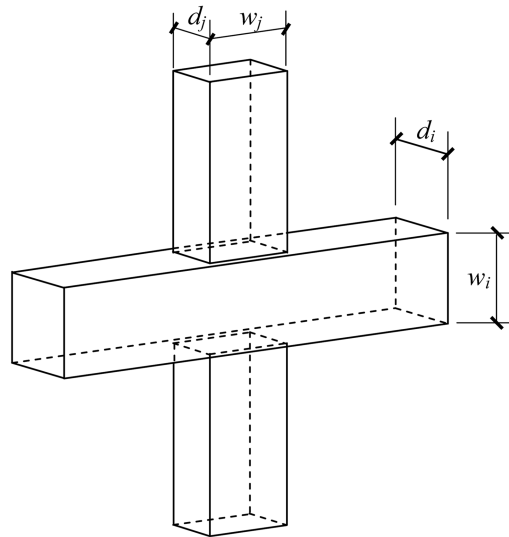


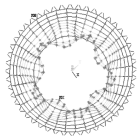
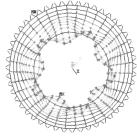
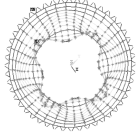
Fig. 6 Detailed figure and geometrical sizes about aero-elastic model node

analysis of the excited response were in good agreement with design requirements, in which the smallest value is 13.67 Hz (the related full-scale value is 0.939 Hz). The damping ratio is about 3.5% which also meets the requirement for reinforced concrete material. Measured results about aero-elastic model are listed in Table 3.

Table 2 Structural dimensions and additional masses for aero-elastic model

Structural member	Height	Radius	Circular sizes		Vertical sizes		Added mass×36 mass
			Thick	Width	Thick	Width	
Ventilation tubing	61.1	336.7	2.8	6.0	6.5	2.8	
	124.1	316.7	0.7	6.0	8.5	0.5	100
	187.0	296.9	0.7	5.5	7.5	0.5	30
	250.0	276.1	0.7	5.0	7.0	0.5	25
	313.0	258.3	0.6	4.5	5.5	0.5	25
	375.9	241.8	0.6	4.5	5.5	0.5	20
	438.9	228.4	0.5	4.0	4.0	0.5	20
	501.9	215.6	0.5	4.0	4.0	0.5	20
	564.9	205.5	0.5	4.0	4.0	0.5	15
	627.8	198.7	0.4	3.5	3.0	0.5	15
	690.8	195.7	0.4	3.5	3.0	0.5	15
	753.8	196.1	0.5	3.5	4.0	0.5	15
	816.8	197.7	0.6	3.5	4.0	0.5	30
	879.7	199.3	0.9	3.5			
Stiffening ring	885.2	199.3	R=0.5 mm steel wire				
Support column	61.1	336.7	R=1.0 mm steel wire				

Table 3 Design parameters and measurement values of cooling tower model

No.	Thin shell model		Beam model		Measured
	Mode shape	Fre. of full-scale Fre. of model	Mode shape	Designed fre. Designed error	Fre. Error ratio
1	 5 circular +2 vertical waves	0.939		14.34	13.67
		13.28		7.98%	2.94%
2	 5 circular +2 vertical waves	1.044		14.35	14.84
		14.76		-2.78%	0.54%
3	 4 circular +2 vertical waves	1.075		13.16	15.43
		15.20		-13.43%	1.51%

### 3. Simulation of Reynolds number effect

The average diameter  $D$  in the middle part along the vertical direction of super-large cooling tower may be about 90.0 m, and design wind velocity  $U$  are usually between 25 m/s and 35 m/s for various engineering fields. From the Reynolds number (Re) expression,  $Re=D \times U/\nu$ ,  $\nu=15E-6m^2/s$ . We know that Re of full-scale cooling towers ranges between  $1.5 \times 10^8$  to  $2.1 \times 10^8$ , while in wind tunnel tests, the number fluctuates from  $2.5 \times 10^5$  to  $3.5 \times 10^5$ . This discrepancy between full-scale and wind tunnel conditions is too large to be ignored reasonably. Usually, the difference of the Reynolds number between test and prototype can be overcome with modification of the model surface roughness (Goudarzi and Sabbagh-Yazdi 2008), and the simulation targets about surface flow parameters, such as Maximum and Minimum pressure values and its angles, zero pressure angle, separation angle, Strouhal number, etc., can be referred to on-site measurement of full-scale cooling towers (DL/T 5339-2006 and GB/T 50102-2003). In accordance with Chinese wind loading Codes, surface pressure distribution under post critical Reynolds condition is suggested as,

$$\mu_p(\theta) = \sum_{k=0}^m a_k \cos k\theta \quad (1)$$

in which,  $\theta$  is the angle,  $m=7$ ,  $a_k$  is the fitting parameter ( $a_0=-0.4426$ ,  $a_1=0.2451$ ,  $a_2=0.6752$ ,  $a_3=0.5356$ ,  $a_4=0.0615$ ,  $a_5=-0.1384$ ,  $a_6=0.0014$ ,  $a_7=0.0650$ ). The distribution curve was suggested by on-site measurement of two full-scale cooling towers with height of about 120 m in the 1980's, and some key parameters about average pressure function around cross section of cooling tower are listed in Table 4.

With the aid of sticking paper belts (10 mm width  $\times$  0.1 mm depth, see Fig. 3(a)) along vertical direction and adjusting incoming wind velocity, the actual aerodynamic characteristics of archetype cooling towers are successfully re-illustrated in the reduced-scale model with lower Reynolds number, see Fig. 7(a). By measuring the tail flow velocity behind the cooling tower model with high-frequency anemometer, the main vortex shedding frequency through frequency-spectrum transformation of aerodynamic time history is obtained at 2.411 Hz (see Fig. 7(b)). The Strouhal number based on the vortex shedding frequency of wake flow is 0.235, larger than 0.2, hence meeting the requirement of cooling tower reduced-scale models.

### 4. Extreme pressure distribution

Based on stochastic process theory, the possible extreme value of a set of stochastic data serials

Table 4 Characteristics of surface average pressure distribution

Maximum pressure and its angles	$C_{P,\max} = 1.0$ , $\theta_{\max} = 0^\circ$
Minimum pressure and its angles	$C_{P,\max} = -1.627$ , $\theta_{\min} = \pm 70^\circ$
zero pressure angle	$\theta_{\text{zero}} = \pm 33^\circ$
separation angle	$\theta_{\text{separation}} = \pm 120^\circ$
Strouhal number	$S_t \geq 0.22$
Average pressure of wake flow	$C_{P,\text{wake flow}} \approx -0.4$

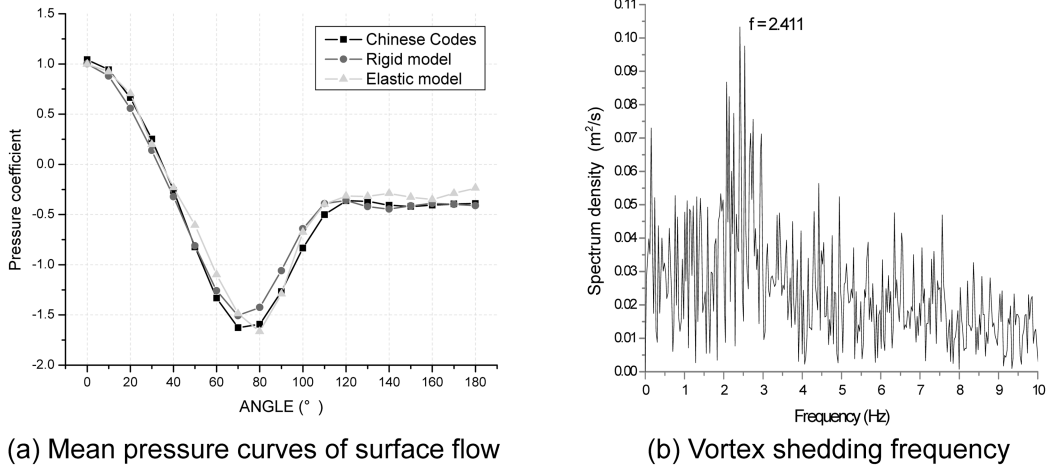


Fig. 7 Simulation of post critical Reynolds effect in reduced-scale models

can be defined by multiply of some basic parameters. The extreme aerodynamic pressure distribution can be formulated in such expression as below:

$$\mu_p = \mu_m + \sigma_\mu \times g \times \rho \tag{2}$$

in which,  $\mu_p$ ,  $\mu_m$  and  $\sigma_\mu$  are extreme value, mean value and RMS value of pressure shape coefficient,  $g$  is peak factor,  $\rho$  is correlation coefficient between general along-wind or cross-wind force history and each pressure tap time-variant series.

Based on wind tunnel pressure measured tests for single tower and correlation technique (Eq. (2)), the extreme value distributions for internal and external pressures around the circular direction of the tower are shown in Fig. 8.

Using the least-square method and triangle series expression, like Eq. (1), the fitting curve about

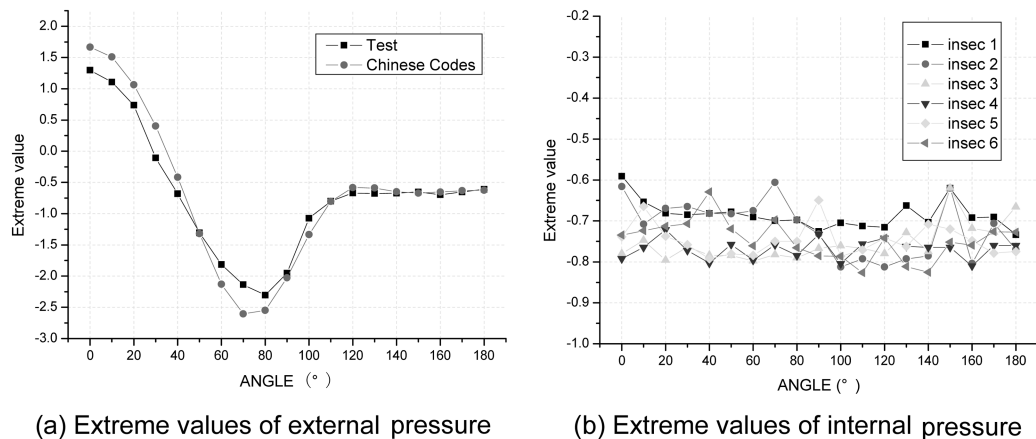


Fig. 8 Extreme value pressure distribution of the cooling tower

external pressure distribution may be gained, with  $m=7$ ,  $a_0=-0.7789$ ,  $a_1=0.3126$ ,  $a_2=1.0159$ ,  $a_3=0.7366$ ,  $a_4=0.0439$ ,  $a_5=-0.1429$ ,  $a_6=0.0742$ ,  $a_7=0.0856$ , see Fig. 8(a). There is an obvious difference between Maximum and Minimum pressure value from the suggested values by Chinese Codes (2003, 2006), since Chinese Codes only adopt a uniform peak factor of 1.6 for Type A terrain. In fact, the analysis process using correlation technique mentioned above utilizes multiple peak factors for different parts along the circular direction, see Eq. (2). For the sake of simplicity, while wind pressure on top of the cooling tower is defined as reference standard, internal pressure can be expressed approximately with uniform distribution curves, see Fig. 8(b), which are determined by incoming flow type and ventilation ratio of stuffing layers at the bottom of the cooling tower. For commonly-used 30% ventilation ratio case, the mean and extreme value pressure coefficient are  $-0.546$  and  $-0.764$  for smooth flow condition,  $-0.409$  and  $-0.573$  for turbulent flow.

## 5. Vibration characteristics of single tower

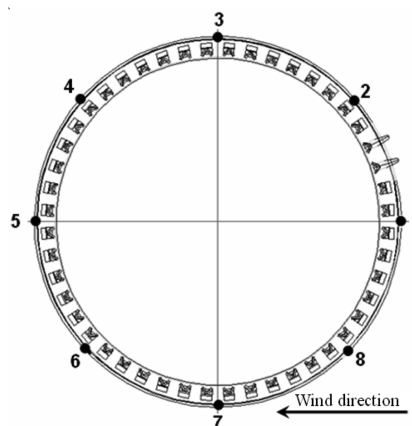
There are eight laser displacement sensors fixed on horizontal tray which moves along the vertical direction for six measurement heights. For each level, the wind-induced displacements can be measured simultaneously (Fig. 9).

The realistic values about peak factor usually lie between 3.5 and 4.5 for wind-excited performance. While analyzing wind-vibration factors of cooling tower, the average peak value factor is predefined as 4.0. Since the parts nearby the bottom of cooling tower are stiffer, the wind-excited mean displacements are so smaller that the wind-vibration factors related to very small mean displacement are not representative, so the wind-induced mean displacement of 10 cm is selected as threshold value. Only if the mean value of wind-vibration response exceeds the threshold value, the wind-vibration factors are taken into consideration.

For the aero-elastic model, the circumferential deformation of the horizontal section and vertical displacement distributions nearby the maximum horizontal displacement profile I-I and II-II are presented in Fig. 10, in which profile I-I is the onward and backward cross-section along the height



(a) Short view on top of cooling tower



(b) Serial number of laser sensors for each level

Fig. 9 The aero-elastic model of cooling tower and laser sensors

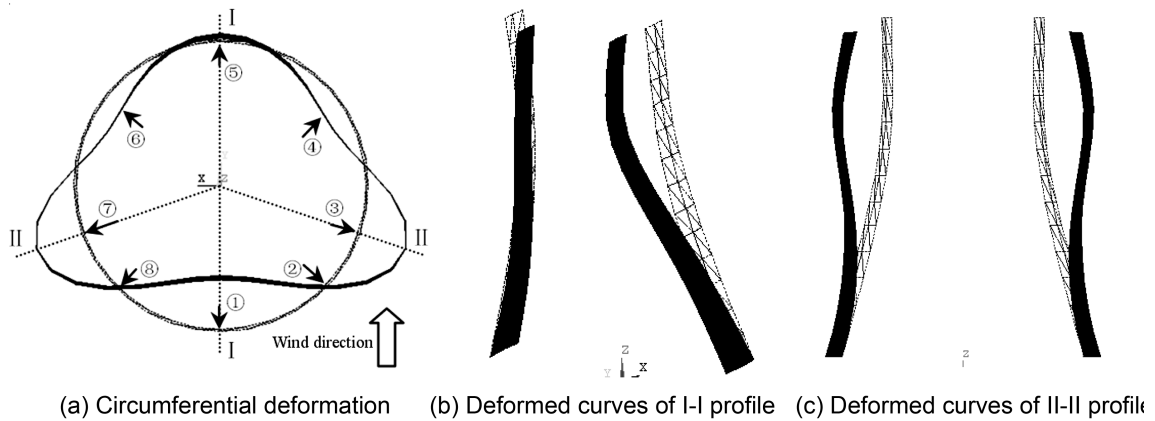


Fig. 10 Displacement distribution of cooling tower aero-elastic model

direction of cooling towers, and profile II-II is lateral cross-section with the angle of about  $\pm 67.5^\circ$  from the incoming wind direction. The maximum displacement is located in the vicinity of windward and lateral parts that are from  $\pm 70^\circ$  to  $\pm 90^\circ$  angle to incoming direction. The response results over the 10 cm threshold value of single tower in Type A terrain are listed in Table 5. In Fig. 11, along the circumferential direction about the throat section (in No.5 section, see Fig. 5), the ratio results concerning pressure shape coefficient, wind-vibration mean value and RMS value are also illustrated.

The above results show clearly that larger wind-induced displacement appears in the upper half of the cooling tower, especially the wind-vibration displacement close to the throat section of cooling tower. Along the circumferential taps, the maximum displacement locates in the incoming taps, the second largest ones are lateral taps which are at about  $\pm 70^\circ$  to  $\pm 90^\circ$  angle from incoming wind direction. The average displacement value is about 10-20 cm. The other smaller response value is about 5 cm. The average wind-induced factor for these taps over the threshold value is 1.70 (see Table 5), which is very close to wind-induced factor 1.60, as suggested by Chinese Codes (2003, 2006) on Type A terrain.

Under the A, B, C, D typical field terrains, aero-elastic model tests have also been conducted for the single cooling tower. More wind-induced factors results for different average displacements and

Table 5 Wind-vibration response for single tower

Section ID	Tap ID	Displacement (cm)			Wind-vibration factor
		Mean	RMS	Max	
6	1	12.248	2.166	20.912	1.71
6	3,7	10.048	2.436	19.792	1.97
5	1	18.024	2.790	29.184	1.62
5	3,7	10.686	2.248	19.678	1.84
4	1	18.098	1.974	25.994	1.44
4	3,7	10.028	1.548	16.220	1.62
3	1	10.346	1.768	17.418	1.68
Total mean		12.783	2.133	21.314	1.70

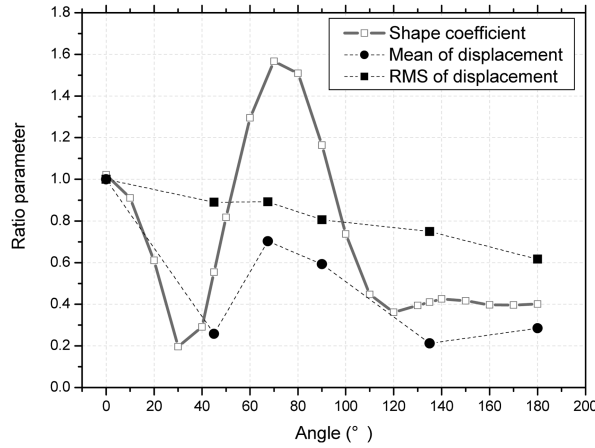


Fig. 11 Circumferential distributions of wind pressure and wind-induced responses on throat section

taps are listed in Table 6. Since wind vibration factors are related to average wind-induced displacement, two types of displacement are accordingly adopted: for windward and lateral taps maximum mean value of 10-15 cm, other taps average of 5-10 cm. From the Table 6, for the larger average response results (10-15 cm), wind vibration factors of windward taps are usually less than those of lateral taps. For the various types of terrain conditions, wind vibration factors of incoming taps show large variation, on the contrary, those of lateral taps are relatively stationary. For the lesser average response (5-10 cm) taps, wind vibration factors obviously exceed those with large

Table 6 Wind vibration factors for typical A, B, C, D terrain fields

Threshold value	Section ID	Tap location	Terrain type			
			A	B	C	D
10~15cm	6	Windward	1.71	1.77	1.82	1.94
	5		1.62	1.67	1.73	1.83
	4		1.44	1.50	1.54	1.64
	3		1.68	1.74	1.79	1.91
	Mean value		1.61	1.67	1.72	1.83
10~15cm	6	Lateral wind	1.97	1.97	1.97	1.98
	5		1.84	1.85	1.85	1.86
	4		1.62	1.63	1.63	1.64
	Mean value		1.81	1.82	1.82	1.83
5~10cm	6	Others	2.34	2.37	2.38	2.52
	5		2.34	2.32	2.52	3.29
	4		2.06	2.19	2.35	2.07
	3		1.90	2.12	2.12	2.51
	Mean value		2.16	2.25	2.34	2.60
Codes value (DL/T 5339-2006)			1.60	1.90	2.30	None

average displacement (10-15 cm). Totally, wind vibration factors show the opposite tendency with increasing average displacement, and it is closely related with average wind vibration response and location on the cooling tower.

### 6. Disturbing effects about two grouped towers

There are totally three types of wind tunnel testing states with respect to two grouped towers aero-elastic model, namely, disturbing towers located in the front, back and at the side of measured one. The scale of wind tunnel flow field is 1:200 on Type A terrain.

The general map is listed in Fig. 12. The ratio of tower distance to base diameter is 1.0~3.5, and the increment values about distance are 5 cm and 10 cm, respectively. The throat section (No.4 section) is selected as measured target.

In Figs. 13-14, the variance about wind-induced extreme value displacement and vibrating factors

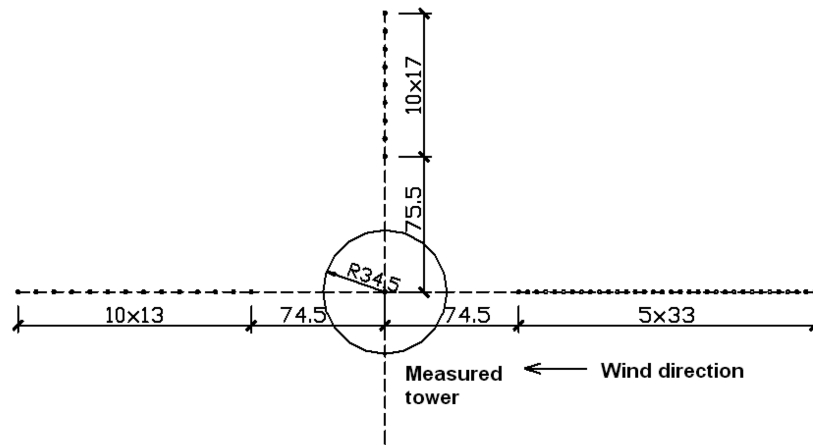


Fig. 12 General map of two grouped towers tests (1:200)

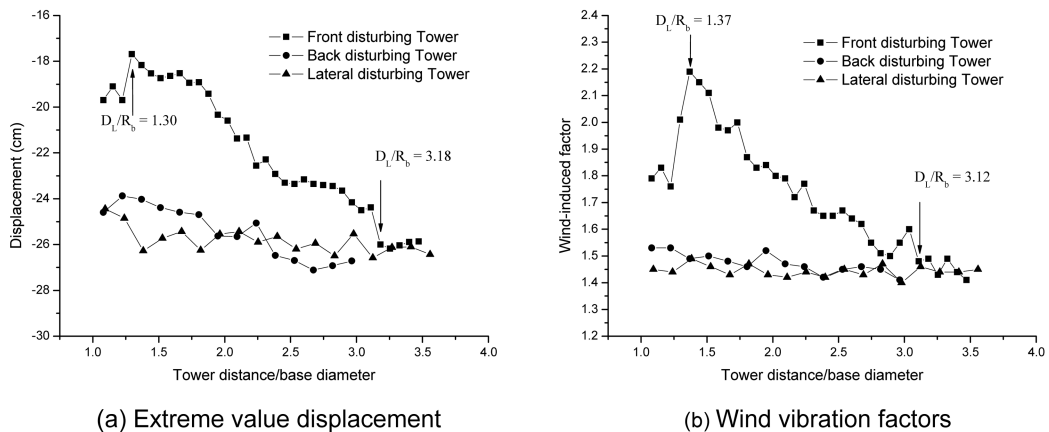


Fig. 13 Disturbing curves of two grouped towers on windward parts (No.1 tap)

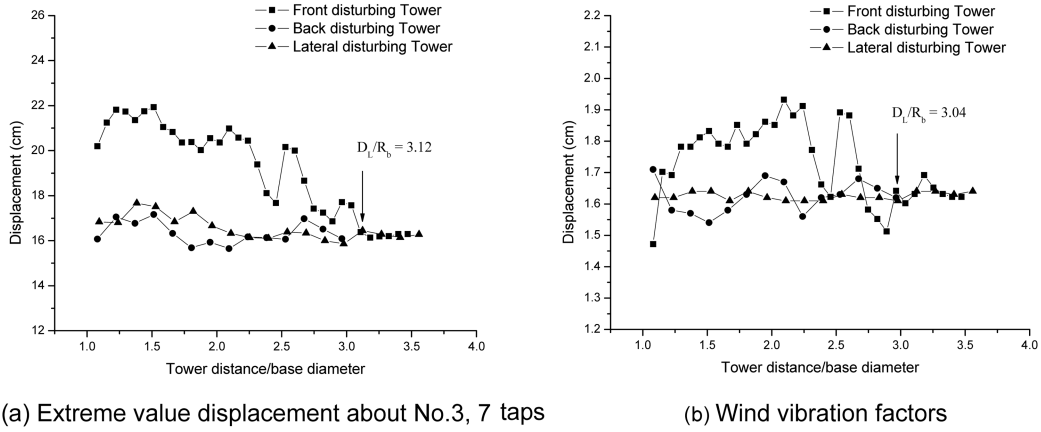


Fig. 14 Disturbing curves of two grouped towers concerning lateral wind (No.3,7 tap)

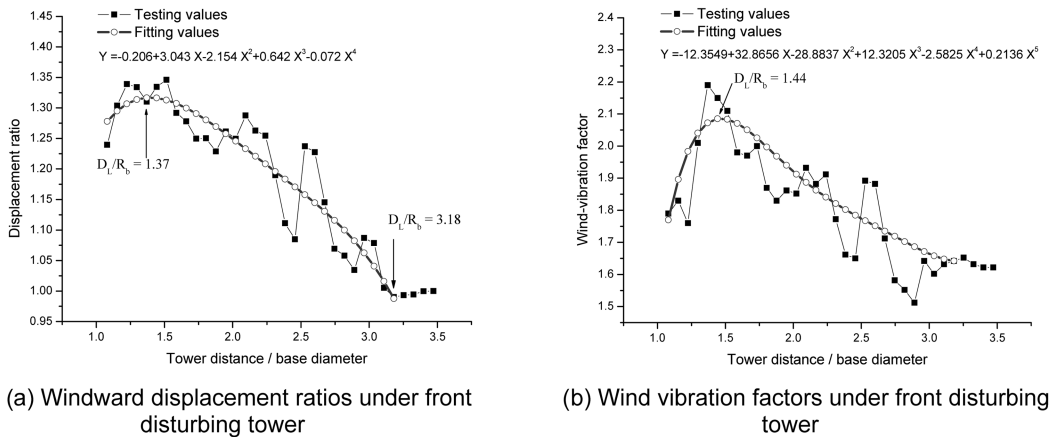


Fig. 15 Fitting curves concerning two grouped towers interference effects

with different tower distance are illustrated. It's clear that the disturbing effect decreases with larger tower distance. While disturbing tower is situated in the front of the measured one, the disturbed effect is the most noticeable. On the contrary, for other two type disturbing locations, the disturbing effect is so small that could be overlooked safely. Fitting curves in relation to two grouped towers interference effects are showed in Fig. 15. If the ratio of tower distance to base diameter  $D_L/R_b \geq 3.18$ , the disturbing effects can also be neglected as well. In other word, the measured tower should be treated as single tower condition safely. While  $D_L/R_b \approx 1.37$  or 1.44, the maximum displacement ratio of 1.32 and wind vibration factor of 2.09 are to be reached.

In Table 7, which illustrates measured results of two grouped tower disturbing tests, when  $D_L/R_b$  ranges within 1.37~1.44, the peak value is obtained, the ratio of wind-induced displacement  $K_d$  about two grouped tower and single tower turns to 1.32, at the same time, the wind-induced factor  $\beta$  is 2.08. While  $D_L/R_b \geq 3.18$ , the measured wind-induced factor of 1.64 is very close to the Chinese Code result of 1.60 for the Type A terrain.

Table 7 Interference effects of two grouped towers

$D_L/R_b$	$K_d$	$\beta$
1.08	1.27	1.77
1.37~1.44	1.32	2.08
1.5	1.31	2.08
2.0	1.25	1.91
2.5	1.16	1.77
3.0	1.06	1.67
$\geq 3.18$	1.00	1.64

## 7. Effects of surrounding geographic and building topography

With the help of aerodynamic pressure measurements, three types of testing states were carried out in  $0^\circ$ - $360^\circ$  wind angle range with  $15^\circ$  angle increment, including single tower in Type A terrain turbulent field, grouped towers in II and III construction stages (see Fig. 1).

In order to get equivalent magnificent coefficient  $K_m$  while taking into account the interference from group towers and other adjacent buildings, the expression is proposed as:

$$K_m = \frac{(C_{F, \max, \text{single}} \times K)(1.0 \times R)}{C_{F, \text{mean, single, code}} \times \beta_{\text{single, code}}} \quad (3)$$

in which  $C_{F, \max, \text{single}}$  is the integration of extreme value of along wind static coefficient for single tower under different wind angles in turbulent flow field,  $K$  is ratio parameter between grouped towers considering interference effects,  $R$  is the percentage item that indicates ratio of inertia force and surface aerodynamic loads,  $C_{F, \text{mean, single, code}}$  is the integration of mean value of along-wind static coefficient from the Chinese Codes,  $\beta$  is the wind vibration factor from the Chinese Codes;

$$C_F(t) = \frac{\sum_{i=1}^n C_{F_i}(t) A_i \cos(\theta_i)}{A_T} \quad (4)$$

in which  $A_i$  is the overlapped area about the  $i_{\text{th}}$  tap,  $\theta_i$  is the angle between the  $i_{\text{th}}$  tap vertical direction and wind axial direction, and  $A_T$  is the total projected area between cooling tower structure and wind axial direction.

A series of tests of surface pressure and wind-induced dynamic response (see Fig. 3) are implemented under II and III construction stage conditions. Incoming wind angle is in the range of  $0^\circ$ - $360^\circ$  with  $15^\circ$  increment, counterclockwise positive from east.

For two grouped tower case in the II stage, the worst condition is for 2# tower under  $195^\circ$  wind angle,  $K_m = 1.238$ , see Fig. 16(a); for four grouped tower case in the III stage, the worst condition is for 4# tower under  $195^\circ$  wind angle,  $K_m = 1.398$ , see Fig. 16(b). Both of  $K_m$  and wind vibration factor exceed values suggested by the Chinese Codes, which requires  $K_m = 1.0$  for standard tower distance and wind vibration factor reaches 1.6 for Type A terrain, indicating strong interference from grouped towers and other adjacent buildings.

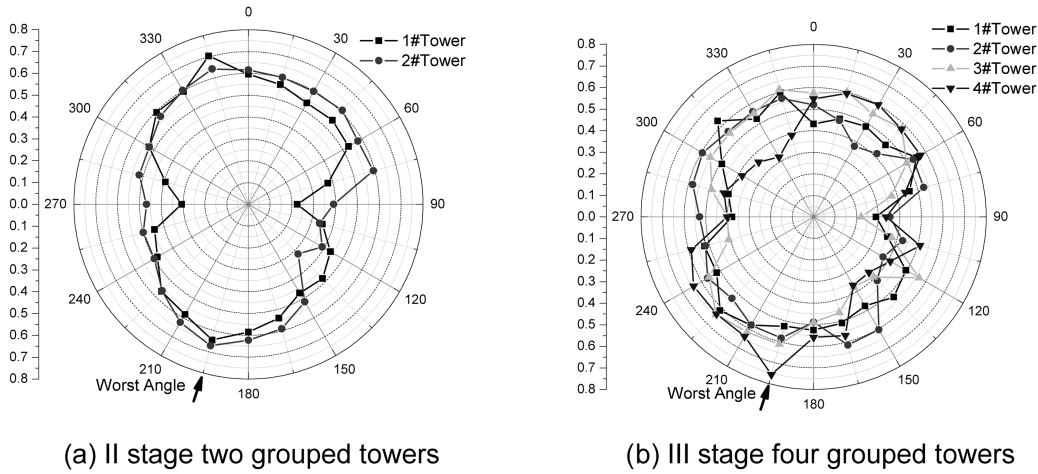


Fig. 16 Along wind static coefficients distributions for various incoming wind angles

The central tower distance under II and III stage conditions, 1.5 and 3.0 times of base diameter, satisfies the minimum tower distance requirement which can ignore the grouped tower effects considering Chinese or BTR Codes. Under the 195° wind angle, several disturbing towers are located along the lateral direction, considering the testing results of two grouped tower distance modification (see Fig. 17), a conclusion can thus be drawn that the measured tower could not be affected by other towers, in Table 8, the two and four grouped tower combination without neighboring buildings and topography, the displacement maximum value and wind vibration factor are very close to testing result of single tower, which can also support the conclusion. Under the worst incoming wind angle (195°) for II, III stages including neighboring buildings and topography, the testing results from aero-elastic model tests and pressure-measured model tests obviously exceed the corresponding values of single tower. By comparison, the interference effects about other neighboring buildings and topography could not be ignored.

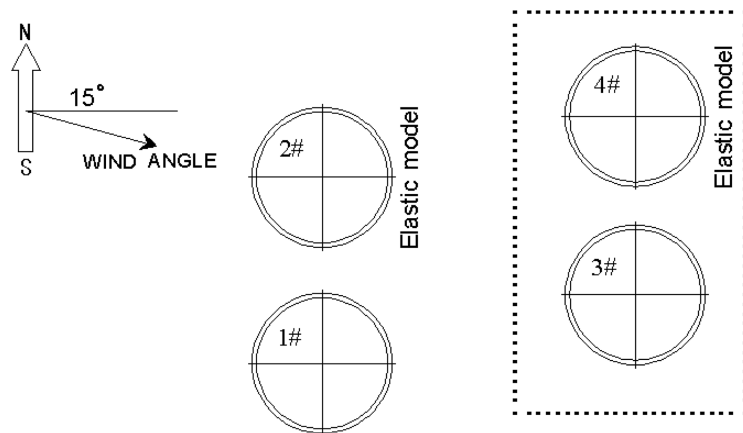


Fig. 17 Two and four grouped towers combination

Table 8 Interference effects testing results

Tests condition	Maximum displacement (cm)	$\beta$	$K_D$
Single tower/Smooth field	20.402	1.37	1.000
Single tower/A type field	21.314	1.70	1.000
Group/195° angle/II stage	25.141	1.74	1.238
Group/195° angle/III stage	29.012	2.17	1.398
Two tower/195° angle	20.843	1.69	
Four tower/195° angle	21.876	1.75	

## 8. Conclusions

The several typical model tests of cooling towers have been investigated in the wind tunnel. The following summarizes the major findings and conclusions of this study:

1. Statistical correlation analysis on external extreme pressure distribution indicates that wind loading Codes of cooling towers seem to be conservative, while the role of internal pressure should be further emphasized.

2. The magnification of neighboring buildings with comparable sizes is very significant, with magnification value well between 1.2~1.4.

3. From the above testing results, corresponding items for minimum tower distance and disturbing effect from wind loading Codes need to be modified and further research works are needed.

The above conclusion, especially about extreme pressure distribution of correlation analysis, should be justified by on-site measurement of full-scale super-large cooling tower, and more investigation be focused on time-variant aerodynamic pressure besides average pressure curves around the tower.

## Acknowledgements

The authors would like to gratefully acknowledge the supports of the National Science Foundation of China (90715039, 2008ZX06004-001 and 50978203). The dedication and efforts of postgraduate students, P.F. Li, L.S. Xu, and Z.K. Wu are highly appreciated.

## References

- Almannai, A., Basar, Y. and Mungan, I. (1981), "Basic aspects of buckling of cooling-tower shells", *J. Struct. Div.*, **ST3**, 521-534.
- Armitt, J. (1980), "Wind loading on cooling tower", *J. Struct. Div.*, **ST3**, 623-641.
- BTR VGB'Richtlinie Bautechnik bei Kühltürmen (1990), *VGB Technische Vereinigung der Großkraftwerksbetreiber e.V.*, Essen.
- Cole, P.P., Abel, J.F. and Billington, D.P. (1975), "Buckling of cooling-tower shells: state-of-the-art", *J. Struct. Div.*, **ST6**, 1185-1203.
- DL/T 5339-2006 (2006), *Code for hydraulic design of fossil fuel power plants*, Development and Reform

- Commission, P.R.C.  
GB/T 50102-2003 (2003), *Code for design of cooling for industrial recirculating water*, Ministry of Construction, P.R.C.
- Goudarzi, M.A. and Sabbagh-Yazdi, S. (2008), "Modeling wind ribs effects for numerical simulation external pressure load on a cooling tower of KAZERUN power plant-IRAN", *Wind Struct.*, **11**(6), 479-496.
- Langhaar, H.L., Boresi, A.P., Miller, R.E. and Bruegging, J.J. (1970), "Stability of hyperboloidal cooling tower", *J. Eng. Mech. Div., Proc. of the American Society of Civil Engineers*, EM5, 753-779.
- Mungan, I. (1976), "Buckling stress states of hyperboloidal shells", *J. Struct. Div.*, **ST10**, 2005-2020.
- Noh, H.C. (2006), "Nonlinear behavior and ultimate load bearing capacity of reinforced concrete natural draught cooling tower shell", *Eng. Struct.*, **28**, 399-410.
- Noorzaei, J., Naghshineh, A., Abdul, M.R., Thanoon, W.A. and Jaafar, M.S. (2006), "Nonlinear interactive analysis of cooling tower–foundation–soil interaction under unsymmetrical wind load", *Thin-Wall. Struct.*, **44**, 997-1005.
- Niemann, H.J. (1980), "Wind effects on cooling tower", *J. Struct. Div.*, **ST3**, 643-661.
- Niemann, H.J. and Köpper, H.D. (1998), "Influence of adjacent buildings on wind effects on cooling towers", *Eng. Struct.*, **20**(10), 874-880.
- Orlando, M. (2001), "Wind-induced interference effects on two adjacent cooling towers", *Eng. Struct.*, **23**, 979-992.
- Règles Professionnelles applicable à la Construction des Réfrigérants Atmosphériques en Béton Armé (1980), Texte Provisoire, SNBATI.
- Sun, T.F. and Gu, Z.F. (1995), "Interference between wind loading on group of structures", *J. Wind Eng. Ind. Aerod.*, **54/55**, 213-225.
- Viladkar, M.N., Karisiddappa, Bhargava, P. and Godbole, P.N. (2006), "Static soil–structure interaction response of hyperbolic cooling towers to symmetrical wind loads", *Eng. Struct.*, **28**, 1236-1251.
- Waszczyszyn, Z., Pabisek, E., Pamin, J. and Radwan'ska, M. (2000), "Nonlinear analysis of a RC cooling tower with geometrical imperfections and a technological cut-out", *Eng. Struct.*, **22**, 480-489.
- Zahlten, W. and Borri, C. (1998), "Time-domain simulation of the non-linear response of cooling tower shells subjected to stochastic wind loading", *Eng. Struct.*, **20**(10), 881-889.